

# MUON G–2: AN INTERPLAY BETWEEN BEAM DYNAMICS AND A MUON DECAY EXPERIMENT AT THE PRECISION FRONTIER\*

M. J. Syphers<sup>†1</sup>, Northern Illinois University, DeKalb, USA  
<sup>1</sup>also at Fermi National Accelerator Laboratory, Batavia, USA

## Abstract

The Muon  $g-2$  Experiment at Fermilab (E989) uses the high proton flux delivered by the Fermilab accelerator complex and an improved detector apparatus to measure the anomalous magnetic moment of the muon to unprecedented precision. In addition to the increased statistics beyond the most recent measurement, the experiment relies on detailed understanding of the incoming muon beam properties as well as the beam dynamics in the experiment's storage ring for proper assessments of systematic errors in the data analysis. Modeling and measurements of beam and storage ring properties, from proton targeting to muon storage, produce a unique unification of particle beam physics with a high energy physics experiment.

## EXPERIMENTAL TECHNIQUE

### The Magnetic Moment Anomaly

The magnetic moment of a particle can be written in terms of its spin as  $\vec{\mu} = g(e/2m)\vec{S}$  and Dirac's relativistic theory predicted a value of  $g = 2$  for fermions. However, measurements have long indicated anomalies in the value of  $g$ , indicated by  $a = (g - 2)/2$ , which take on particle-dependent values. The anomaly for the muon, for example, has a value of  $a_\mu \approx 0.001166$ .

The precession of a charged particle in an electromagnetic field is governed by the Thomas-BMT equation [1], yielding a spin precession frequency:

$$\vec{\omega}_s = -\frac{e}{m} \left[ \left( a + \frac{1}{\gamma} \right) \vec{B} - a \left( \frac{\gamma}{\gamma + 1} \right) (\vec{\beta} \cdot \vec{B}) \vec{\beta} - \left( a - \frac{1}{\gamma^2 - 1} \right) \frac{\vec{\beta} \times \vec{E}}{c} \right] \quad (1)$$

The spin components are those in the frame of the particle and the field components are in the lab frame. The difference between this precession frequency and the cyclotron frequency,  $\omega_c$ , will produce conditions to arrive at a value of the anomaly. In the experiment, vertical focusing is performed using electrostatic quadrupole fields and with the central momentum of the beam chosen to be the "magic momentum" (roughly 3.09 GeV/c) where the last term in Eq. 1 is zero, then with an ideal trajectory that is perpendicular to the magnetic field direction we find that  $a = m\omega_a/eB$ ,  $\omega_a \equiv \omega_s - \omega_c$ . The energies and arrival time of the positrons

coming from the decay of the stored muons are measured by calorimeters. The direction of motion of the highest energy positrons will be highly correlated with the spin direction of the original muon. Thus, the rate at which a detector station will observe these positrons will "wiggle" with the muon precession frequency and, with 24 detector stations about the circumference, hundreds to thousands of decay positron measurements can be made each fill. The number of detected positrons will vary with time roughly as

$$N(t) = N_0 e^{-t/\tau_\mu} [1 + A \cos(\omega_a t + \phi_0)] \quad (2)$$

where  $\tau_\mu$  is the lifetime of the muon in the lab,  $A$  is the amplitude of the "wiggle" and  $\phi_0$  is an initial phase. A variety of signal analyses provide determinations of  $\omega_a$ .

The most recent measurement of  $a_\mu$  was provided by Experiment E821 at Brookhaven National Laboratory [2], which shows a discrepancy with today's theoretical estimate at the  $\sim 3.5\sigma$  level, providing the impetus to embark on a new measurement with yet higher precision.

## THE FERMILAB EXPERIMENT

As the Tevatron program was nearing its completion, the antiproton production and storage system infrastructure was viewed as a possible location for future low energy experiments at Fermilab. By re-purposing one of the triangular-shaped antiproton storage rings and associated beam lines, a scenario was developed for producing beams for a new  $g-2$  experiment at Fermilab (experiment E989) as well as a muon-to-electron conversion experiment (E973). Fig. 1 shows the present "Muon Campus"; the smaller white building in the center of the photo contains the new Muon  $g-2$  experiment. Through an accelerator improvement project [3] the Fermilab injector system has been upgraded to be able to generate pulses of 8 GeV kinetic energy proton beam from the Booster at a full 15 Hz rate. During a 1.4 s period, 12 15-Hz cycles are used to fill the Main Injector for neutrino beam operation,



Figure 1: Fermilab Muon Campus providing production and transport of muons to E989. Photo courtesy of Fermilab.

\* This manuscript has been authored by Fermi Research Alliance, LLC under Contract No. DE-AC02-07CH11359 with the U.S. Department of Energy, Office of Science, Office of High Energy Physics.

<sup>†</sup> msyphers@niu.edu

and remaining cycles can be used to provide 8 GeV beam to other experiments. The Muon  $g-2$  experiment uses four of these cycles to generate up to 16 pulses, each 120 ns long, of  $10^{12}$  protons onto a target station. Secondary pions are collected with a momentum selection of roughly 3.1 GeV/c and sent toward the re-purposed Delivery Ring (foreground of Fig. 1). After four revolutions the slower protons that remain can be removed with a kicker system. The reduction of pion and proton content in the beam was a major design goal to reduce hadronic flash at injection. By this point, the remaining secondary beam – predominately muons – is sent to the storage ring with roughly 95% polarization. Details of the Fermilab experiment and technique can be found in [4].

## THE MUON BEAM

### Modeling Efforts

As new beam lines were laid out and an existing storage ring was reconfigured as a decay channel, particle rates and beam properties for the experimental conditions were predicted from modeling of protons interacting with the existing Fermilab antiproton target and the subsequent capture and transport of secondary particles downstream. The roughly 2.5 km system from target to the Muon  $g-2$  storage ring has been modeled extensively, including very detailed aperture information and alignment data. From the original studies,  $10^6$  muons were expected to reach the storage ring per  $10^{12}$  protons on target, with an rms momentum spread of roughly  $\pm 1\%$  and polarization  $\sim 95\%$ . Details can be found in [5].

### Early Commissioning

The modeling efforts of the beam production were very successful, with the muon beam meeting expectations. While the overall rate continues to improve, the beam emittances, beam profiles, momentum spread and polarization at the end of the transport system are all as predicted from the initial beam modeling using standard particle production and transport codes. Details of the commissioning results can be found in [6–8].

## THE STORAGE RING

Fig. 2 shows the 7 m radius muon storage ring of E989. The beam region of the storage ring contains a vertical magnetic field, uniform to less than  $\sim 1$  ppm when integrated about the circumference and across the aperture. A field measurement system routinely delivers a detailed mapping of the field quality about the circumference and provides input into the beam simulations. Details of the ring field and its measurement system can be found in [9].

### Modeling Efforts

With details of the incoming muon beam, measured ring field imperfections, modeled electrostatic quadrupole fields and kicker field and waveform measurements, the beam behavior and subsequent detector rates are simulated and compared with measurements. As noted above, a detector’s rate will depend upon the precession of the polarized

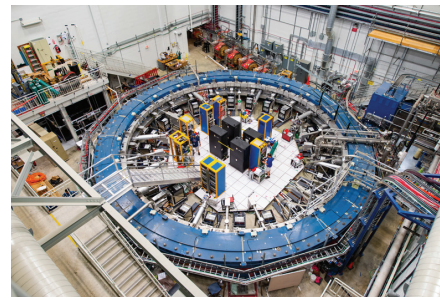


Figure 2: E989 Muon  $g-2$  ring. Photo courtesy of Fermilab.

muon beam, but the rate will also depend upon several beam dynamical effects as well. For instance residual coherent betatron oscillations and quadrupole oscillations of the beam envelope from the injection process will affect the detector rates. Likewise, the large momentum spread of the incoming beam will cause longitudinal de-bunching as well as transverse chromatic detuning; a large dispersion mismatch between the injection line and the ring also plays a major role. All of these effects manifest themselves in the detector rates and come into play during data reduction and analysis. Details of the injection process and typical signals can be found in [10].

**Momentum Distribution** An important measurement, as discussed further below, is that of the equilibrium momentum distribution of the stored muons. Modeling efforts using a variety of codes and techniques are used to track muons into the ring and ascertain their survivability. For instance, with a momentum acceptance of roughly  $\pm 0.5\%$ , the storage ring will only accept the “core” of the momentum distribution provided by the beam line. This relatively uniform distribution will be shaped by the circular aperture of the storage region which has ever-smaller acceptance for larger deviations in momentum from the central (“magic”) value. The momentum distribution is reconstructed for each injection pulse. A mismatched injection kick, for example, creates a large injection error and an asymmetric equilibrium momentum distribution can be formed. Fig. 3 compares the results of a phase space analysis from modeling with a corresponding processed detector data.

**Loss Rate Modeling** All muons injected will eventually be lost, mostly through the decay process. However, some

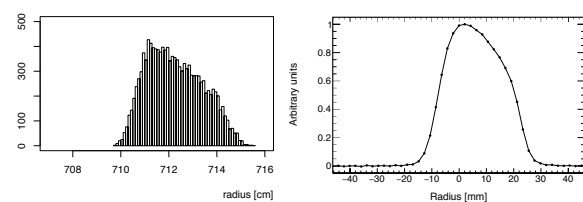


Figure 3: Momentum distribution from modeling [L] and corresponding result (preliminary) [R] from detector data [R] using technique described in [10].

Content from this work may be used under the terms of the CC BY 3.0 licence (© 2019). Any distribution of this work must maintain attribution to the author(s), title of the work, publisher, and DOI

muons are destined to be lost prior to decay through other means, such as beam-gas interactions or diffusion through resonant processes due to field imperfections. In some cases it takes several hundred revolutions for a muon to simply reach the aperture after it is injected. If such losses are correlated with certain properties of the beam, such as momentum or betatron amplitudes, and if such properties also contain correlations to the spin of the particle, then it is possible for a systematic error of the spin precession frequency to be present in the final analysis. The ring vacuum is at the level of  $10^{-6}$  torr or better and loss rates due to beam interactions with the residual gas is negligible over the 500  $\mu$ sec time scale of a store. Particle loss rates as a function of betatron tunes are much more important and have been modeled and measured, with major resonances being clearly identified. By appropriate scraping during the injection process, beam loss rates (not due to decay) can be reduced to the level of 0.1% per muon lifetime when far from betatron resonances. For details of the modeling of losses due to resonances, see [12].

## SYSTEMATIC ERRORS

To reach an overall measurement error of 0.14 ppm on the value of  $a_\mu$ , beam related systematic errors must be held to sub-ppm levels for each of several categories. Some of the more important ones are listed below.

### *Oscillations and Decoherence*

The overlap of the decay positron phase space with the acceptance of the detectors provides a time varying signal on top of the desired “wobble” in the detector rate. The injection process generates a coherent betatron oscillation at the betatron tune as well as an envelope oscillation at twice the tune (both horizontal and vertical). In addition, the coherence of the oscillation will decrease due to chromaticity and from nonlinearities in the electrostatic quadrupole field. Detailed knowledge and understanding of these frequencies and the observable effects from the beam dynamics are required for the detailed analyses of the raw detector signals.

### *Pitch and Electric Field*

From Eq. 1, the spin will precess about the direction of motion due to the  $(\vec{\beta} \cdot \vec{B})\vec{\beta}$  term, which is governed by the electrostatic focusing. We find that upon averaging over time and over the distribution, vertical betatron oscillations generate a necessary *correction* to the precession (pitch correction) of amount  $\Delta\omega_a/\omega_a \approx -\frac{1}{4} \langle y^2 \rangle / \beta_y^2$ , where here  $\beta_y$  is the vertical amplitude function of the ring. Hence, the vertical beam distribution is carefully reconstructed for each store. Similarly, the third term comes into play significantly due to the momentum distribution. Since the electric field varies linearly with position, and since the closed orbits vary linearly with momentum, then the average electric field experienced by a particle goes like  $\Delta\omega_a/\omega_a \approx -2\langle x_e^2 \rangle / (D_x \beta_x)$ , where  $D_x$  and  $\beta_x$  are the horizontal dispersion and amplitude functions, respectively, and  $\langle x_e^2 \rangle$  is determined from the reconstructed momentum distribution as described above.

Detailed modeling helps to reduce the errors on these corrections to tolerable levels.

### *Lost Muons*

Of the muons reaching the storage ring 95% are lost at injection. Of the remaining muons, 10% have trajectories that will eventually encounter an aperture if they do not decay beforehand. If these 10% have different spin correlations than the other 90%, a systematic *apparent* frequency shift can be observed during the loss process. Detailed modeling of the particle phase space including spin is being performed to disentangle this systematic effect.

### *Operational Beam Physics*

In addition to the important systematic error analyses described above, beam physics modeling of muon delivery and storage have helped the collaboration understand operational and commissioning issues, such as the shakedown of injector kicker performance, bad resistors leading to undesirable time constants on the electrostatic quadrupoles, and misalignments of various elements.

## FUTURE OUTLOOK

The Muon  $g-2$  experiment is searching for evidence of non-Standard Model physics and possible energy scales by measuring the magnetic moment anomaly of the muon to an unprecedented level. The second run of the experiment is underway, having already acquired more data than in the BNL E821 experiment and with much more data in the pipeline. Recent improvements to the injection kicker system, beam line adjustments and overall operational tuning will allow the experiment to reach its goals.

The detector system of E989 provides very accurate detection of decay particle trajectories and energies and the experiment relies heavily on beam dynamics to interpret its physics signals. Improvements to beam physics calculations and analysis techniques are leading to further reductions to systematic errors in the experimental procedure. A new feature in the muon beam development is the introduction of a material “wedge” in a dispersive region of the beam transport system, which is reducing the momentum spread in order to enhance the muon density in the central momentum region of the storage ring.

The Muon  $g-2$  experiment is an application of beam physics and technology to measure precisely a property of a fundamental particle that can be computed equally precisely by the Standard Model. The precision being sought by the experiment is heavily reliant upon the basic physics of particle beams and provides a unique opportunity for beam physicists to play a major role in a frontier science experiment.

## ACKNOWLEDGEMENTS

The author would like to thank the many members of E989 leading to this report and to Fermilab, the U.S. Department of Energy, and Northern Illinois University for their support.

## REFERENCES

- [1] V. Bargmann, L. Michel, and V. L. Telegdi, "Precession of the Polarization of Particles Moving in a Homogeneous Electromagnetic Field", *Phys. Rev. Lett.* **2**, 435 (1959).
- [2] G.W. Bennett, *et al.*, (Muon g-2 Collaboration) *Phys. Rev. D* **73**, 072003 (2006).
- [3] W. Pellico, K. A. Domann, F. G. Garcia, K. E. Gollwitzer, K. Seiya, and R. M. Zwaska, *FNAL - The Proton Improvement Plan (PIP)*, in *Proc. 5th Int. Particle Accelerator Conf. (IPAC'14)*, Dresden, Germany, Jun. 2014, pp. 3409–3411. doi:10.18429/JACoW-IPAC2014-THPME075
- [4] J. Grange, *et al.*, "Muon g2 Technical Design Report," Fermi National Accelerator Laboratory, Batavia, IL, USA, FERMILAB-FN-0992-E (2015); arXiv:1501.06858 [physics.ins-det].
- [5] D. Stratakis, *et al.*, "Accelerator performance analysis of the Fermilab Muon Campus", *Phys. Rev. Accel. and Beams* **20**, 111003 (2017).
- [6] D. Stratakis, B. Drendel, J.P. Morgan, M.J. Syphers, N.S. Froemming, "Commissioning and first results of the Fermilab Muon Campus", *Phys. Rev. Accel. and Beams* **22**, 011001 (2019).
- [7] J. Bradley, B. Drendel, D. Stratakis "First measurement of traverse beam optics for the Fermilab Muon Campus using a magnet scanning technique", *Nucl. Inst. and Meth. in Physics Research, A* **903** (2018) 3237.
- [8] D. Stratakis, B. Drendel, J. Morgan, N. Froemming, M.J. Syphers, "Commissioning and First Results of the Fermilab Muon Campus", presented at the 10th International Particle Accelerator Conf. (IPAC19), Melbourne, Australia, May, 2019, paper MOZZPLM3, this conference.
- [9] M. W. Smith, "Developing the Precision Magnetic Field for the E989 Muon  $g - 2$  Experiment," PhD diss., University of Washington, Seattle (2017) doi:10.2172/1431565.
- [10] D. L. Rubin, *et al.*, "Muon Beam Dynamics And Spin Dynamics In The G-2 Storage Ring", in *Proc. 9th Int. Particle Accelerator Conf. (IPAC18)*, Vancouver, BC, Canada, Apr.-May 2018, pp. 5029-5034. doi:10.18429/JACoW-IPAC2018-FRXGBE2.
- [11] Preliminary data provided by A. Chapelain, private communication.
- [12] D. Tarazona, M. Berz, K. Makino, "Muon loss rates from betatron resonances at the Muon  $g-2$  Storage Ring at Fermilab", presented at the 10th International Conference on Charged Particle Optics (CPO-10), Key West, Florida, October. 2018.